Neutron capture cross sections of ^{136,138,140,142}Ce and the decays of ^{137}Ce

S. Torrel and K. S. Krane
Department of Physics, Oregon State University, Corvallis, Oregon 97331, USA
(Received 10 July 2012; revised manuscript received 27 August 2012; published 27 September 2012)

The activation method has been used to measure the cross sections for radiative capture of neutrons by all isotopes of stable Ce (mass numbers 136, 138, 140, and 142). Both the thermal cross sections and the resonance integrals have been determined from separate irradiations with thermal and epithermal neutrons, wherever possible cross-checking results from different irradiation facilities with different flux distributions. Because determination of precise cross sections by activation requires equally precise values of the decay half-lives, we have remeasured decay half-lives of ^{137}Ce^{g}, ^{137}Ce^{m}, ^{139}Ce^{m}, ^{141}Ce, and ^{143}Ce. Improved values for the energies and intensities of the γ rays in the decays of ^{137}Ce^{g} and ^{137}Ce^{m} have also been determined, along with corresponding values for the β-decay feedings and energies of excited states in ^{137}La.

DOI: 10.1103/PhysRevC.86.034340 PACS number(s): 25.40.Lw, 27.60.+j, 23.20.Lv

I. INTRODUCTION

A systematic study of neutron capture by the stable Ce isotopes at stellar energies by Käppeler *et al.* [1] revealed inconsistencies in the accepted data set as well as important systematics among the measured values, especially in the approach to the semimagic ^{140}Ce ($N = 82$). A similarly systematic study of neutron capture in Ce at low and intermediate energies has not yet been done. There is fair agreement in the literature [2,3] on the capture cross sections for ^{140,142}Ce, but there is a lack of similar data for capture by ^{136,138}Ce. Moreover, the interesting question of the relative cross sections for capture leading to the low-spin ground states and high-spin isomeric states in ^{137,139}Ce has not been addressed by the existing data set. A systematic understanding of the neutron cross sections by Ce isotopes is also necessary for calculating neutron propagation in reactors, because Ce isotopes are produced in large quantities in the fission of ^{235}U.

The present work reports the results of a systematic study of the neutron capture cross sections for the stable Ce isotopes, in analogy with a similar study recently completed in our laboratory of the cross sections of the stable Ba isotopes [4]. In particular, we have focused in this work on a careful determination of the cross sections for the production of the ground and metastable states in ^{137,139}Ce. It is especially important in these studies to correct for capture by epithermal neutrons in determining the cross section for thermal neutrons, because the resonance integral is often an order of magnitude larger than the thermal cross section. We have therefore undertaken measurements of both the thermal cross sections and the resonance integrals, which are reported in the present work. We also report new measurements of the half-lives for several of the Ce decays, along with an improved set of values for the γ-ray energies and intensities in the decays of ^{137}Ce^{g} and ^{137}Ce^{m} and the consequences for the properties of the excited states of ^{137}La.

II. EXPERIMENTAL DETAILS

For the cross section measurements, samples of CeO_2 powder of natural isotopic abundance ranging from 10 to 150 mg were irradiated in the Oregon State University TRIGA reactor [5]. Four different irradiation facilities were used: a thermal column (TC; nominal thermal and epithermal neutron fluxes of respectively 9.0×10^{10} and 2.0×10^{8} neutrons cm^{-2} s^{-1}), an irradiation site in the reactor core's outer or G ring (GRICIT; 4.3×10^{12} and 3.9×10^{11} neutrons cm^{-2} s^{-1}), a cadmium-lined irradiation tube in the central core (CLICIT; 0 and 1.2×10^{12} neutrons cm^{-2} s^{-1}), and a fast pneumatic transfer facility ("rabbit"; 8.3×10^{12} and 3.3×10^{11} neutrons cm^{-2} s^{-1}). Some rabbit samples were enclosed in a Cd box (1 mm wall thickness) to isolate the epithermal neutrons.

To monitor the neutron flux, each irradiation was accompanied by several samples of known cross sections. Samples of Au and Co as dilute (respectively 0.134% and 0.438%) alloys in thin Al metal foils served as primary flux monitors. The thermal cross section and resonance integral of Au were assumed to be respectively 98.65 ± 0.09 b and 1550 ± 28 b and those of Co to be respectively 37.18 ± 0.06 b and 74 ± 2 b [2]. Zr served as a secondary flux monitor, especially for correcting for the small epithermal components in the TC and rabbit facilities. Irradiations for the cross section measurements typically lasted 1–3 h in the GRICIT, CLICIT, and TC facilities, and counting began about 4 h after the irradiations. Irradiations in the rabbit facility were of duration 1–2 min, and counting began a few minutes after the irradiations.

The γ rays were observed with a high-purity Ge detector (nominal volume of 169 cm^3, efficiency of 35% compared with NaI at 1332 keV, resolution of 1.68 keV at 1332 keV). Source-to-detector distances for the cross section measurements were generally 10 to 20 cm, for which coincidence summing effects are negligible. The signals were analyzed with a digital spectroscopy system connected to a desktop computer. Peak areas of the γ-ray lines, which were well isolated from neighboring peaks, were determined with the ORTEC MAESTRO software [6].

Parameters used in the analysis of the Ce cross sections are shown in Table I. Isotopic abundances are taken from the current recommended values of the IUPAC Commission on Isotopic Abundances and Atomic Weights [7]. Decay half-lives are from the Evaluated Nuclear Structure Data File (ENSDF)

TABLE I. Properties of Ce isotopes for cross section analysis.

Capture by	Capture to	Abundance (%)	Half-life	Analyzing γ rays
^{136}Ce	^{137}Ce^{g}	0.185(2)	9.11(3) h	447.2 (1.69%)
	^{137}Ce^{m}		34.80(3) h	254.3 (11.1%)
^{138}Ce	^{139}Ce^{g}	0.251(2)	137.64(2) d	165.9 (79.9%)
	^{139}Ce^{m}		57.58(32) s	754.2 (92.5%)
^{140}Ce	^{141}Ce	88.45(5)	32.508(13) d	145.4 (48.3%)
^{142}Ce	^{143}Ce	11.11(5)	33.039(6) h	293.3 (42.8%)

[8] for ^{139}Ce^{g}, ^{141}Ce, and ^{143}Ce, with the remainder being new values deduced from the present work. Branching ratios of the γ rays are from the ENSDF. The branching ratio for the 447.2-keV γ ray in the decay of ^{137}Ce^{g} is derived from the present spectroscopy results (discussed below) and agrees with the value from the most recent ENSDF compilation.

After correcting for the decay of the sample and the γ-ray branching and efficiency factors, the deduced activities were analyzed according to the result of solving the rate equation for a simple capture and decay process, for which the activity a is

$$a = N(\sigma\phi_{\text{th}} + I\phi_{\text{epi}})(1 - e^{-\lambda t_{\text{i}}}), \tag{1}$$

where N (assumed to be constant) is the number of stable Ce target nuclei in the irradiated sample, ϕ_{th} and ϕ_{epi} are the thermal and epithermal neutron fluxes, σ and I are respectively the effective thermal cross section and resonance integral, and t_{i} is the irradiation time. In the cases in which the radioactive ground state is fed through the metastable state (^{137}Ce and ^{139}Ce), the ground-state population resulting from the isomeric decays was subtracted out, so that the quoted cross sections for the ground states represent direct production from neutron capture.

Because there are no broad or low-lying neutron resonances known for any of the Ce isotopes considered in the present work, the cross section closely follows the $1/v$ behavior below about 1 eV. Therefore the effective thermal cross section characterizes the entire thermal region. (This is equivalent to setting Wescott's g factor equal to unity [9].) The effects of neutron absorption within the samples are also negligible, given the thin samples used in the present experiments.

The effective resonance integral I includes a small contribution from the $1/v$ region. Assuming the Cd cutoff energy to be about 0.5 eV, this contribution amounts to about 0.45σ; the corrected resonance integral I' is then

$$I' = I - 0.45\sigma. \tag{2}$$

The resonance integral is generally much larger than the thermal cross section, in which case this amounts to a small correction that is at most one standard deviation of I. For ^{141}Ce and ^{143}Ce the resonance integral is comparable to the thermal cross section, so for those cases Eq. (2) produces a large correction to the measured value of I (25%–50%).

Several factors contribute to the uncertainties in the cross sections: isotopic abundance, half-life, flux determinations (including corrections of thermal cross sections for the presence of epithermal neutrons), detector efficiencies, and decay scheme factors, including γ-ray branching. Overall these factors combine to give a typical minimum uncertainty of 4%–5%.

For the ^{137}Ce spectroscopy studies, 2-mg samples of CeO_2 enriched to 30% in ^{136}Ce were irradiated to produce an initial ^{137}Ce^{g} activity of 150 μCi. Counting was done at source-to-detector distances from 10 to 5 cm, moving closer to the detector at intervals of approximately one half-life. This procedure enables sum peaks and long-lived impurities readily to be identified.

The γ-ray spectra were analyzed for peak locations and areas using the fitting code SAMPO [10]. Energy calibrations for the spectroscopy studies were done by counting the Ce samples simultaneously with ^{152}Eu [11]. Efficiency calibrations were done with standardized sources of ^{133}Ba and ^{152}Eu. The calibration below 200 keV was also characterized using reactor-produced sources of ^{160}Tb, ^{169}Yb, and ^{182}Ta.

III. HALF-LIVES AND CROSS SECTION RESULTS

Figure 1 shows a sample γ-ray spectrum just after a rabbit irradiation, illustrating the peaks that appear at short times, and Fig. 2 shows a spectrum of lines from the long-lived activities several hours after a core irradiation.

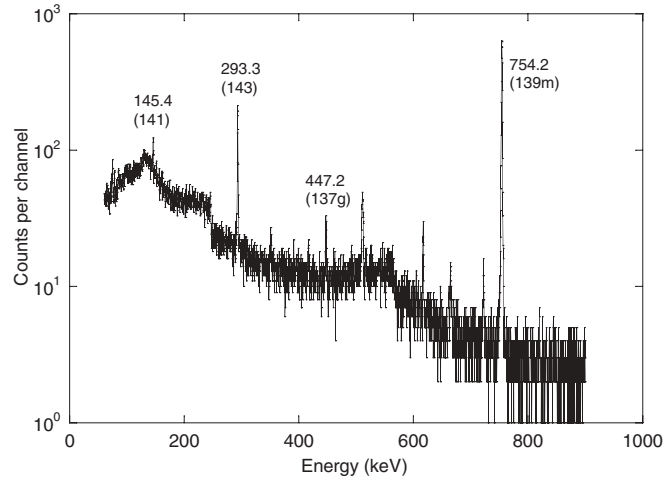

FIG. 1. γ-ray spectrum from short-lived isotopes in irradiated Ce just after rabbit irradiation. Labeled lines were used for cross-section evaluation.

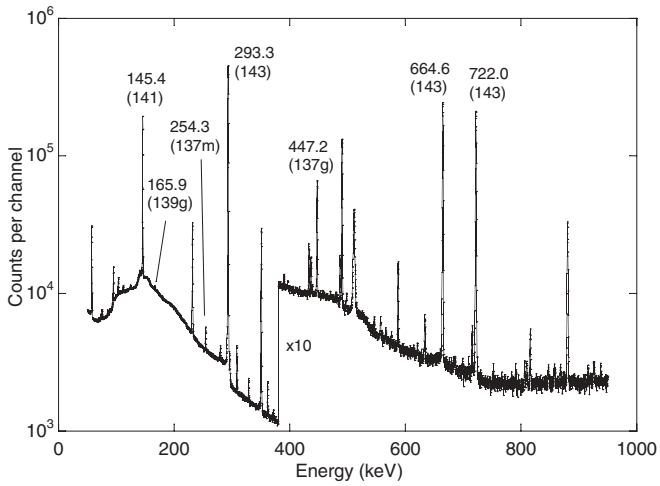

FIG. 2. γ-ray spectrum of irradiated Ce following core irradiation showing lines from longer-lived isotopes used for cross-section evaluation.

A. Half-lives

Before analyzing the cross sections, it is necessary to have precise values for the radioactive decay half-lives. We have remeasured the half-lives of five of the six activities used in the present studies (all except ^{139}Ce^{g}). The deduced values from the present work, where superior to previous values, are presented in Table I. For each half-life measurement, dead-time corrections were checked using either a much longer-lived Ce decay (for example, ^{143}Ce for ^{139}Ce^{m}), an impurity of precisely known half-life present in our samples (for example, ^{140}La), or a long-lived external source (such as ^{60}Co or ^{152}Eu).

^{137}Ce. Previous values of the ^{137}Ce^{g} and ^{137}Ce^{m} half-lives, respectively 9.0 $\pm$ 0.3 h and 34.4 $\pm$ 0.3 h, have been reported only by Danby *et al*. [12] based on a measurement of the 447.2- and 254.3-keV lines from activities following the decay of ^{137}Pr produced from Ce(p,xn) reactions. To our knowledge, there has been no previous report of a half-life determined from a source produced by neutron capture. Our analysis of the 447.2-keV line from ^{137}Ce^{g} for at least three half-lives from several samples, including the separated isotope, gave a half-life of 9.11 $\pm$ 0.03 h. The 254.3-keV isomeric transition from ^{137}Ce^{m} was observed for at least three half-lives from several samples, again including the separated isotope, resulting in a half-life of 34.80 $\pm$ 0.03 h. These values are in agreement with the previously measured ones but are an order of magnitude more precise.

^{139}Ce^{m}. The presently accepted half-life of ^{139}Ce^{m} is 54.8 $\pm$ 1.0 s, based on the value reported by Geiger and Graham [13]. A somewhat larger value, 56.44 $\pm$ 0.48 s, was reported in the same year by Yule [14].We have measured this half-life by following the decay of eight samples to obtain the value 57.58 $\pm$ 0.32 s, slightly larger than the previous values.

^{141}Ce. Our value for this half-life is 32.56 $\pm$ 0.05 d, which is in agreement with but less precise than the accepted value of 32.508 $\pm$ 0.013 d, based on a consensus of a large number of previously measured values [8].

^{143}Ce. From the analysis of several samples during three or more half-lives, we have deduced a value of 33.01 $\pm$ 0.02 h for this half-life. This is in agreement with, but somewhat less precise than, the currently accepted value of 33.039 $\pm$ 0.006 h, based on a measurement reported by Abzouzi *et al*. [15].

TABLE II. Measured values of Ce thermal cross sections.

Process	Thermal cross section σ (b)	
	Present work	Previous work
^{136}Ce $\rightarrow$ ^{137}Ce^{m}	0.344(16)	0.6[a]
^{136}Ce $\rightarrow$ ^{137}Ce^{g}	3.91(18)	6.3[a]
^{138}Ce $\rightarrow$ ^{139}Ce^{m}	0.047(20)	0.007[b], 0.018(5)[c]
^{138}Ce $\rightarrow$ ^{139}Ce^{g}	0.98(5)	1.0[b], 0.65(22)[c], 1.02(12)[d]
^{140}Ce $\rightarrow$ ^{141}Ce	0.51(2)	0.582(5)[d], 0.59(6)[e], 0.54(4)[f]
^{142}Ce $\rightarrow$ ^{143}Ce	0.88(4)	0.967(10)[d], 0.94(9)[f], 0.95(5)[g]

[a]Brosi and Ketelle [16].
[b]Ketelle *et al*. [18].
[c]Sehgal [19].
[d]Heft [21],
[e]Lantz *et al*. [22].
[f]Alstad *et al*. [23].
[g]Roy and Yaffe [27].

B. Cross sections

Given the newly measured values for the half-lives, along with the other data listed in Table I, we can now discuss the results of the cross section measurements. Values for the thermal cross sections are summarized in Table II, and the resonance integrals (including the $1/v$ contribution) are given in Table III.

$^{136}Ce \rightarrow ^{137}Ce$. The thermal cross sections leading to the ^{137}Ce^{m} metastable state were determined from measurements in three facilities (GRICIT, TC, and rabbit), and the resonance integrals from two measurements (CLICIT and Cd-shielded rabbit). Good agreement was obtained from the various measurements, and the average values for the isomeric cross sections are

$$\sigma = 0.344 \pm 0.016 \text{ b}, \quad I = 5.5 \pm 0.3 \text{ b}.$$

The cross sections leading to the ^{137}Ce^{g} ground state were determined from the analysis of the 447.2-keV line. Its intensity was first corrected for the competing 446.0- and 447.5-keV lines from the ^{143}Ce decay. After also correcting for the population of the ground state that originates from the isomer (using the deduced cross sections for formation of the isomer), the cross sections for direct production of the ground state were deduced to be

$$\sigma = 3.91 \pm 0.18 \text{ b}, \quad I = 63.5 \pm 3.1 \text{ b}.$$

The only previous report of these cross sections was given by Brosi and Ketelle [16], who estimated values of the respective thermal cross sections of the isomer and ground state to be 0.6 and 6.3 b. The ratio of the isomeric and total (ground state + isomeric) cross sections was measured by Gangrsky *et al*. [17] to be 0.15 $\pm$ 0.01, in rather poor agreement with the value 0.081 $\pm$ 0.005 obtained from the cross sections deduced in the present work.

TABLE III. Measured resonance integrals of Ce.

Process	Resonance integral I (b)	
	Present work	Previous work
^{136}Ce → ^{137}Ce^{m}	5.5(3)	
^{136}Ce → ^{137}Ce^{g}	63.5(31)	
^{138}Ce → ^{139}Ce^{m}	1.95(10)	1.21(13)[a]
^{138}Ce → ^{139}Ce^{g}	8.6(5)	6.7(31)[b]
^{140}Ce → ^{141}Ce	0.55(2)	0.483(5)[b], 0.43(2)[c], 0.48(5)[d], 0.49(5)[e], 0.25(3)[f], 0.48(5)[g]
^{142}Ce → ^{143}Ce	1.25(6)	1.66(15)[b], 1.10(6)[c], 1.6(2)[e], 0.73(4)[f]

[a]Van der Linden *et al*. [20].
[b]Heft [21].
[c]Van der Linden *et al*. [26].
[d]Lantz *et al*. [22].
[e]Alstad *et al*. [23].
[f]Ricabarra *et al*. [24] (reduced value I').
[g]Steinnes [25].

$^{138}Ce \rightarrow ^{139}Ce$. Owing to its short half-life, the ^{139}Ce^{m} cross sections could be obtained only from measurements with the rabbit facility. After irradiating several samples in both the unshielded and Cd-shielded configurations, the deduced cross sections for formation of the metastable state are

$$\sigma = 0.047 \pm 0.020 \text{ b}, \quad I = 1.95 \pm 0.10 \text{ b}.$$

The large relative uncertainty of the thermal value is a result of the extreme sensitivity of this small cross section to the uncertainty of the resonance integral when correcting for the effect of the epithermal neutrons on the measurement in the unshielded configuration.

For the ground state, measurements of the thermal cross section from three different facilities (GRICIT, TC, rabbit) and of the resonance integral from two different facilities (CLICIT, Cd-shielded rabbit) yielded (after correction for ground-state production through the isomer)

$$\sigma = 0.98 \pm 0.05 \text{ b}, \quad I = 8.6 \pm 0.5 \text{ b}.$$

The thermal cross sections for formation of the isomer and ground state were previously reported by Ketelle *et al*. [18] (respectively, 0.007 and 1.0 b) and by Sehgal [19] (respectively, 0.018 ± 0.005 and 0.65 ± 0.22 b), the latter value being deduced from a measured ratio between the ^{138}Ce and ^{140}Ce cross sections using an older value for the ^{140}Ce cross section that has been superseded by a current value twice as large. The thermal cross section leading to ^{139}Ce^{m} was deduced by Sehgal in comparison with an unspecified value of the ^{27}Al thermal cross section. Van der Linden *et al*. [20] deduced a value of 1.21 ± 0.13 b for the resonance integral from a measured value for I/σ of 81 ± 9, assuming a value of 0.015 b for σ. Using the larger value of σ (with its large relative uncertainty) obtained from the present results yields a correspondingly larger resonance integral of 3.8 ± 1.6 b from Van der Linden's measurement, which (within its large uncertainty) agrees with the presently measured resonance integral.

A more recent measurement by Heft [21] of the ground-state cross sections (σ = 1.02 ± 0.12 b, I = 6.7 ± 3.1 b) is in agreement with but much less precise than the present results. The ratio of the ground-state and total cross sections reported by Gangrsky [17] (0.025 ± 0.003) is in reasonable agreement with the less precise value 0.046 ± 0.019 from the present results.

$^{140}Ce \rightarrow ^{141}Ce$. Owing to the relatively small resonance integral, it was possible to obtain precise results for the thermal cross section from all three facilities (GRICIT, TC, rabbit), which gave

$$\sigma = 0.51 \pm 0.02 \text{ b}, \quad I = 0.55 \pm 0.02 \text{ b}.$$

Our value for σ is slightly smaller than most of the previous values [21–23] listed in Table II, while our value for I is slightly larger than the previous values [21–26] shown in Table III.

$^{142}Ce \rightarrow ^{143}Ce$. Here again the relatively small resonance integral gives only a small correction for the epithermal neutrons, which does not significantly increase the uncertainty in the thermal cross section deduced from the GRICIT and rabbit facilities. We have obtained consistent thermal cross section values from three facilities, resulting in

$$\sigma = 0.88 \pm 0.04 \text{ b}, \quad I = 1.25 \pm 0.06 \text{ b}.$$

As was the case for ^{140}Ce, the present thermal cross section is slightly smaller than previous values [21,23,27] listed in Table II, while our value for the resonance integral lies between the limits of the values [21,23,24,26] shown in Table III.

IV. γ-RAY SPECTROSCOPY

Figure 3 shows a γ-ray spectrum of a sample of irradiated Ce enriched to 30% in ^{136}Ce. In addition to ^{137}Ce^{g} (150 μCi) and ^{137}Ce^{m} (3 μCi), the sample also contained other Ce isotopes: ^{135}Ce (0.005 μCi, produced from n,2n reactions), ^{139}Ce (0.002 μCi), ^{141}Ce (0.16 μCi) and ^{143}Ce (0.45 μCi), plus small quantities of other rare earths, including ^{140}La, ^{149}Nd, ^{152}Eu^{m}, and ^{153}Sm, and also ^{187}W. These impurities caused only minor interference with the measurement.

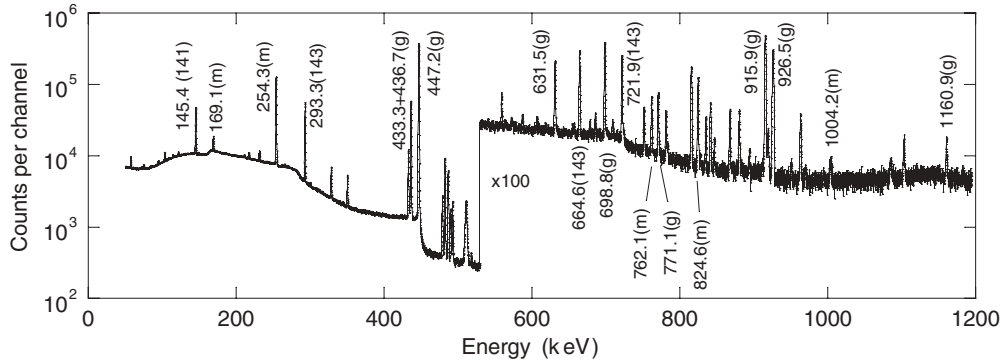

FIG. 3. γ-ray spectrum of irradiated enriched Ce sample. Peaks labeled g and m are respectively from the $^{137}Ce^{g}$ and $^{137}Ce^{m}$ decays. Peaks labeled 141 and 143 are from the ^{141}Ce and ^{143}Ce decays.

The ^{137}Ce sample was counted along with a ^{152}Eu calibration sample for several runs (10 h in total for the $^{137}Ce^{g}$ decays and 42 h for the $^{137}Ce^{m}$ decays) to determine the energies of the stronger γ-ray lines. The sample was counted for an additional 4 d without the calibration sample to study the weaker $^{137}Ce^{g}$ lines without interference from the ^{152}Eu and eventually the $^{137}Ce^{m}$ lines without interference from either $^{137}Ce^{g}$ or ^{152}Eu.

The energy uncertainty associated with the peak fitting is often below 10 eV for lines with more than 10^4 counts, and even including the uncertainties in the energy calibration lines [11] (typically no more than a few eV) would often give a total energy uncertainty below 10 eV. However, we feel that such a small uncertainty is inconsistent with the systematic variations in the energy fits among different data runs and that 10 eV is a more realistic estimate of the minimum uncertainty. The minimum uncertainty in the intensities has been set at 1%, which represents the typical fitting uncertainty of the energy calibrations.

The γ-ray energies and intensities from the decays of $^{137}Ce^{g}$ deduced from the present studies are listed in Table IV along with the values from the most recent Nuclear Data Sheets (NDS) compilation [28], based on the work reported by Henry *et al.* [29]. Overall our data agree with and are significantly more precise than the previous results, typically by an order of magnitude or more in both energy and intensity. A small correction (amounting to 10% at the beginning of the measurement) was necessary to correct the intensity of the 479-keV γ ray for the presence of an unresolved γ ray from ^{187}W.

The γ rays emitted in the decay of $^{137}Ce^{m}$ are summarized in Table V. The weak 917-keV line was partially obscured

TABLE IV. Energies and intensities of γ rays emitted in the decay of $^{137}Ce^{g}$.

Previous work[a]		Present work		Levels[b]	
E (keV)	I	E (keV)	I	Initial	Final
10.61(5)	491(11)			B	A
148.83(8)	0.5(2)	148.897(20)	0.671(20)	E	D
217.03(5)	2.2(3)	217.031(10)	2.18(3)	K	F
433.22(9)	29.1(5)	433.259(12)	29.2(3)	K	D
436.59(9)	149(5)	436.628(10)	150.5(15)	C	B
447.15(8)	1000	447.181(10)	1000(10)	C	A
479.12(10)	6.7(3)	479.158(15)	6.47(6)	K	C
482.47(10)	25.7(9)	482.527(10)	25.6(3)	D	B
493.03(10)	5.9(3)	493.093(10)	5.94(6)	D	A
529.3(2)	0.2(1)	529.65(10)	0.065(10)	M	E
631.38(6)	7.5(4)	631.395(10)	7.65(8)	E	B
678.26(12)	0.5(2)	678.349(21)	0.380(15)	M	D
698.72(11)	17.5(9)	698.713(10)	16.6(2)	F	B
709.30(11)	0.6(1)	709.296(26)	0.526(13)	F	A
724.4(3)	0.4(2)	724.329(50)	0.238(13)	M	C
770.97(10)	3.4(2)	770.945(10)	3.38(3)	H	B
781.57(13)	1.7(2)	781.487(10)	1.63(2)	H	A
915.80(13)	28.9(10)	915.769(10)	29.6(3)	K	B
926.35(13)	19.0(7)	926.310(10)	18.4(2)	K	A
1160.85(22)	0.84(8)	1160.857(10)	0.923(13)	M	B

[a]From Henry *et al.* [29].
[b]See Table VI for identification of levels.

TABLE V. Energies and intensities of γ rays emitted in the decay of $^{137}Ce^{m}$.

Previous work[a]		Present work		Levels[b]	
E (keV)	I	E (keV)	I	Initial	Final
10.61(5)				B	A
87.2(2)	20(3)	87.27(3)	22(2)	L	J
169.26(4)	995(60)	169.254(10)	1090(20)	L	I
254.29(5)	24800(900)	254.283(10)	25700(250)	137m	137g
762.30(10)	435(20)	762.081(10)	433(4)	G	A
824.82(12)	1000	824.765(10)	1000(10)	I	B
835.38(12)	234(10)	835.317(10)	235(2)	I	A
906.84(16)	6.3(11)	906.68(5)	7.0(5)	J	B
917.45(17)	29(5)	917.44(6)	21(3)	J	A
993.81(21)	4.5(6)	994.004(13)	2(2)	L	B
1004.49(20)	51(6)	1004.552(25)	51(1)	L	A

[a]From Henry *et al*. [29].
[b]See Table VII for identification of levels.

in the valley between the stronger lines at 915.8 keV from $^{137}Ce^{g}$ and 919.6 keV from the ^{140}La impurity, so its energy and intensity determinations were subject to relatively large uncertainties. The 994-keV line showed considerable effects of true coincidence summing (169 + 825 keV), amounting to nearly 100% of the observed intensity of this weak line. (The 1005-keV line also showed a smaller effect of summing due to 169 + 835 keV, which amounted to no more than 10% of the observed intensity of the line even at a source-to-detector distance of 5 cm.)

Tables VI and VII show the energy levels in ^{137}La populated in the decays of $^{137}Ce^{g}$ and $^{137}Ce^{m}$. The energy of the 10.553-keV level was determined from the difference between the energies of the cascade and crossover transitions from the 447-, 493-, 709-, 781-, 835-, 926-, and 1005-keV levels. The β-decay intensities have been deduced by comparing the γ-ray intensities populating and depopulating each level. In this calculation we have assumed the NDS value of 97.84 $\pm$ 0.08% for the intensity of the beta decay feeding 10.553-keV level. The uncertainties in the β-decay intensities in the $^{137}Ce^{g}$ decay derive mostly from the uncertainty in the 10.553-keV intensity, with the exception of the β intensity to the 493-keV level, the large relative uncertainty of which results from subtracting two large and comparable values for the populating and depopulating γ-ray intensities.

Based on the γ-ray intensity of the 254-keV isomeric transition from $^{137}Ce^{m}$ measured in the present work and its internal conversion coefficient of 7.93 from the NDS, we obtain a total intensity of 99.24 $\pm$ 0.02% for the isomeric transition and thus 0.76 $\pm$ 0.02% for the β transitions from $^{137}Ce^{m}$ leading to ^{137}La. The uncertainties in the β intensities given in Table VII represent the combination of the uncertainties in the intensities of the ^{137}La γ rays and that of the overall normalization of the total β intensity.

V. DISCUSSION

Neutron capture by the even-mass stable isotopes of Ce (Z = 58) shares many features in common with the same process in Ba (Z = 56) [4]. For several of the isotopes (^{130,132,134,136}Ba and ^{136,138}Ce), neutron capture produces a low-spin ($1/2^+$ or $3/2^+$) ground state and a higher-spin ($9/2^-$ or $11/2^-$) low-lying metastable state. Immediately beyond the N = 82 shell closure (^{138}Ba and ^{140,142}Ce), isomerism is not present. The measured cross sections reinforce these

TABLE VI. Energy levels of ^{137}La populated in the decay of $^{137}Ce^{g}$.

Level	Previous work[a]				Present work		
	E (keV)	J^{π}	$I_{\beta+\varepsilon}$	log ft	E (keV)	$I_{\beta+\varepsilon}$	log ft
A	0.000	$7/2^+$			0.000		
B	10.59(4)	$5/2^+$	97.84(8)	5.37(2)	10.553(7)	97.84(8)	5.376(2)
C	447.17(6)	$5/2^+$	1.95(7)	6.67(2)	447.176(7)	1.96(7)	6.67(2)
D	493.09(6)	$(3/2)^+$	$\approx$0.0018	$\approx$9.6	493.080(7)	0.0014 (7)	9.76(22)
E	641.96(6)	$1/2^+$	0.0134(9)	8.57(4)	641.954(11)	0.0139(5)	8.56(2)
F	709.30(6)	$(3/2)^+$	0.027(2)	8.15(4)	709.277(9)	0.0254(10)	8.18(2)
H	781.57(9)	$(7/2)^+$	0.0086(6)	8.50(4)	781.494(8)	0.0085(3)	8.51(2)
K	926.33(6)	$5/2^+$	0.145(6)	6.90(2)	926.322(6)	0.146(5)	6.90(2)
M	1171.37(10)	$(1/2^+,3/2^-)$			1171.425(10)	0.00271(10)	6.42(6)

[a]From Nuclear Data Sheets compilation [28].

TABLE VII. Energy levels of ^{137}La populated in the decay of ^{137}Ce^{m}.

Level	Previous work[a]				Present work		
	E (keV)	J^{π}	I_{ε}	logft	E (keV)	I_{ε}	logft
A	0.000	$7/2^{+}$			0.000		
B	10.59(4)	$5/2^{+}$			10.553(7)		
G	762.27(10)	$11/2^{+}$	0.197(14)	8.17(4)	762.083(10)	0.188(5)	8.20(1)
I	835.37(8)	$9/2^{+}$	0.08(3)	8.5(2)	835.316(7)	0.037(9)	8.81(11)
J	917.44(11)	$9/2^{+}$	0.007(3)	9.4(2)	917.300(24)	0.0026(15)	9.8(3)
L	1004.62(8)	$11/2^{-}$	0.51(4)	7.38(4)	1004.562(7)	0.532(17)	7.36(2)

[a]From Nuclear Data Sheets compilation [28].

similarities. As the shell closure is approached, the thermal cross sections drop dramatically by an order of magnitude and are then restored to larger values beyond the shell closure.

In interpreting the cross sections, it is instructive to examine the isomeric ratio IR, defined respectively for thermal and epithermal neutrons as

$$IR_{th} = \frac{\sigma_m}{\sigma_g + \sigma_m} \quad \text{and} \quad IR_{epi} = \frac{I_m}{I_g + I_m}. \tag{3}$$

From the thermal cross sections and resonance integrals of the ground and metastable states measured in the present work, we obtain

$$\begin{aligned} 136 \rightarrow 137g,m: \quad IR_{th} &= 0.081 \pm 0.005, \\ IR_{epi} &= 0.080 \pm 0.005, \\ 138 \rightarrow 139g,m: \quad IR_{th} &= 0.046 \pm 0.019, \\ IR_{epi} &= 0.185 \pm 0.012. \end{aligned}$$

A similar analysis for the Ba isotopes from the data of Ref. [4] yields

$$\begin{aligned} 130 \rightarrow 131g,m: \quad IR_{th} &= 0.077 \pm 0.006, \\ IR_{epi} &= 0.098 \pm 0.006, \\ 132 \rightarrow 133g,m: \quad IR_{th} &= 0.084 \pm 0.005, \\ IR_{epi} &= 0.092 \pm 0.006. \end{aligned}$$

A statistical model [30] suggests that the isomeric ratios depend on three factors: the spin of the compound state formed in the capture, a parameter characterizing the width of the distribution of states with that spin, and the average number of prompt γ rays (assumed to be primarily of dipole character) in the cascade connecting the capture states with the ground or isomeric states. In the Ce isotopes considered in the present work and in the Ba isotopes reported in Ref. [4], all targets have a spin of 0. If we assume only s-wave capture, the compound states have only spin 1/2. The small values of IR thus reflect the relative difficulty of connecting the compound states with the metastable state ($\Delta J = 4$ or 5) with a cascade of dipole transitions compared with connecting the compound states with the ground state ($\Delta J = 0$ or 1). In the cases of capture by ^{130,132}Ba and ^{136}Ce, the good agreement among the values of IR and in particular for each nuclide the good agreement between IR_{th} and IR_{epi} suggest that this explanation may have considerable validity. (A similar study by Ledoux *et al.* [31] of captures by eight nuclides with spins J other than 0 likewise showed $IR_{th} \approx IR_{epi}$ in most cases, with the deviant cases explained on the basis of differing populations of the $J \pm 1/2$ compound states and the ensuing differences in the γ-ray cascades leading to the ground and metastable states.) Huizenga and Vandenbosch [30] caution against applying their statistical model as the yields become small, which seems to apply to the present data, as the good agreement between IR_{th} and IR_{epi} is not present for captures by ^{138}Ce for which the thermal cross section is an order of magnitude smaller than that of the other Ce nuclides. If, for example, s-wave capture is suppressed, then even a small admixture of p-wave captures by epithermal neutrons will enhance the value of IR_{epi} relative to IR_{th}. On the other hand, isomeric ratios deduced from cross sections measured for capture by the spin-0 nuclides of Sn and Te show reasonably consistent values for thermal and epithermal neutrons even as the thermal cross sections decrease to a few millibarns [32,33].

Because deducing the cross sections through activation measurements depends critically on the measured values of various parameters (such as γ-ray branchings and half-lives), it is important to check the activation results against those of other methods. Table VIII shows such a comparison between the present values of the thermal cross sections and the results of measurements based on the intensities of the prompt γ rays that populate the various Ce levels [34]. Overall the agreement is quite satisfactory with the exception of ^{139}Ce^{g}. The explanation for this discrepancy is not apparent.

The low-lying structure of ^{137}La is built on the $7/2^{+}$ ground state and $5/2^{+}$ first excited state, presumably identified respec-

TABLE VIII. Comparison of Ce thermal cross sections from activation and from primary γ rays.

Final nuclide	Thermal cross section σ (b) deduced from	
	Activation[a]	Primary γ rays[b]
^{137}Ce^{m}	0.344(16)	0.20(6)
^{137}Ce^{g}	3.91(18)	3.8(4)
^{139}Ce^{m}	0.047(20)	
^{139}Ce^{g}	0.98(5)	6.1(4)
^{141}Ce	0.51(2)	0.284(17)
^{143}Ce	0.88(4)	0.732(23)

[a]Present work.
[b]Firestone *et al.* [34].

TABLE IX. Cascade-to-crossover ratios in ^{137}La.

Level (keV)	J^π	Cascade-to-crossover ratio		
		β decay	$(p,2n)$[a]	$(^{11}B,4n)$[b]
447.2	$5/2^+$	0.151(2)	0.15(2)	
493.1	$(3/2)^+$	4.31(7)	4.3(6)	
709.3	$(3/2)^+$	31.6(8)	30(9)	
781.5	$(7/2)^+$	2.07(3)	2.0(3)	
835.3	$9/2^+$	4.26(6)	3.7(6)	2.5(4)
917.3	$9/2^+$	0.33(5)	0.17(4)	
926.3	$5/2^+$	1.61(2)	1.3(3)	
1004.6	$11/2^-$	0.04(4)	0.10(4)	

[a]Reference [35].
[b]Reference [36].

tively with the $g_{7/2}$ and $d_{5/2}$ shell model orbitals expected to be occupied by the 57th proton. Other low-lying excited states may in turn be identified with shell model states, including $d_{3/2}$ (493 or 709 keV), $s_{1/2}$ (642 keV), or $h_{11/2}$ (1005 keV). The first vibrational state in the neighboring isotones ^{136}Ba and ^{138}Ce occurs at about 800 keV, making it likely that others of the levels listed in Tables VI and VII are associated with particle-plus-phonon states involving the $g_{7/2}$ and $d_{5/2}$ orbitals. The relative intensities of the γ rays from a given level to the ground and first excited states should thus serve as a probe of the $g_{7/2}$ and $d_{5/2}$ content of that level. The intensity ratios of the cascade ($J^\pi \rightarrow 5/2^+$) and crossover ($J^\pi \rightarrow 7/2^+$) transitions for the ^{137}La levels determined in the present decay studies are listed in Table IX. The possibility of unresolved transitions from other levels influencing these results can be discounted by comparing the decay results with those from other studies, notably in-beam γ-ray intensity measurements following nuclear reactions, which would in general be expected to produce relative level populations different from those of the decay studies. Table IX compares the cascade-to-crossover ratios from the present work with those of ^{137}La levels populated in $(p,2n)$ reactions in a study by Kortelahti *et al.* [35] and in $(^{11}B,4n)$ reactions in the work reported by Chanda *et al.* [36]. Overall the agreement is quite good, particularly in the case of the 781-keV level, whose properties have been subject to competing interpretations. Henry *et al.* [29] suggested an assignment of $3/2^+$ or $5/2^+$ based on the $\log ft$ value, and the $\log ft$ value deduced from the present work is consistent with that conclusion. However, Kortelahti *et al.* [35] report a coincidence between the 169 keV ($1005 \rightarrow 835$) and 771 keV ($781 \rightarrow 11$) transitions, which suggests a 54-keV transition connecting the 835 and 781 keV levels. Such a transition has not yet been observed in either the decay or reaction studies, but Kortelahti assume it must be of $M1$ multipolarity and thus assign $7/2^+$ to the 781-keV level. However, such an assignment would require that the ^{137}Ce^g β decay to the 781-keV level be second forbidden, which is in complete disagreement with the observed $\log ft$ of 8.5—the intensity of a second forbidden decay would be expected to be reduced by about four orders of magnitude relative to the observed value. The good agreement between the decay and reaction data on the branching ratios involving the 781-keV level offers no suggestion of a second level at that energy, nor does the excellent match between the level energy obtained in the present work from the direct transition to the ground state (781.489 ± 0.010 keV) and the cascade transition through the first excited state (781.500 ± 0.012 keV). A second level at that energy would likely show a different cascade-to-crossover ratio that might in turn have different effects on the fits to the two peaks and produce an energy mismatch. Also, two levels at nearly the same energy would be populated differently in the ^{137}Ce^g and ^{137}Ce^m decays, causing a shift in the peak energy with time due to the differing half-lives; no such effect appears in our data within the 10-eV uncertainty of the peak fits.

ACKNOWLEDGMENTS

The support of the staff and facilities of the Oregon State University Radiation Center in carrying out these experiments is acknowledged with gratitude.

[1] F. Käppeler, K. A. Toukan, M. Schumann, and A. Mengoni, Phys. Rev. C **53**, 1397 (1996).
[2] S. F. Mughabghab, *Atlas of Neutron Resonances: Resonance Parameters and Thermal Cross Sections Z = 1 − 100* (Elsevier, Amsterdam, 2006).
[3] EXFOR/CSISRS Experimental Nuclear Reaction Data, National Nuclear Data Center, Brookhaven National Laboratory, http://www.nndc.bnl.gov/exfor/exfor00.htm.
[4] A. Y. Dauenhauer and K. S. Krane, Phys. Rev. C **85**, 064301 (2012).
[5] http://radiationcenter.oregonstate.edu/.
[6] ORTEC, Inc., http://www.ortec-online.com/pdf/a65.pdf.
[7] M. Berglund and M. E. Wieser, Pure Appl. Chem. **83**, 397 (2011).
[8] Evaluated Nuclear Structure Data File, National Nuclear Data Center, Brookhaven National Laboratory, http://www.nndc.bnl.gov/ensdf/.
[9] C. H. Wescott, W. H. Walker, and T. K. Alexander, in *Proceedings of the Second United Nations International Conference on the Peaceful Uses of Atomic Energy*, Vol. 16 (United Nations, Geneva, 1958), p. 70.
[10] P. A. Aarnio, J. T. Routti, and J. V. Sandberg, J. Radiol. Nucl. Chem. **124**, 457 (1988).
[11] R. G. Helmer and C. van der Leun, Nucl. Instrum. Methods Phys. Res. A **450**, 35 (2000).
[12] G. T. Danby, J. S. Foster, and A. L. Thompson, Can. J. Phys. **36**, 1487 (1958).
[13] J. S. Geiger and R. L. Graham, Can. J. Phys. **45**, 2281 (1967).
[14] H. P. Yule, Nucl. Phys. A **94**, 442 (1967).
[15] A. Abzouzi, M. S. Antony, and V. B. Ndocko Ndongue, J. Radiol. Nucl. Chem. **137**, 381 (1989).
[16] A. R. Brosi and B. H. Ketelle, Phys. Rev. **103**, 917 (1956).
[17] Yu. P. Gangrsky, P. Zuzaan, N. N. Kolesnikov, V. G. Lukashik, and A. P. Tonchev, Bull. Russ. Acad. Sci. **65**, 121 (2001).

[18] B. H. Ketelle, H. Thomas, and A. R. Brosi, Phys. Rev. **103**, 190 (1956).
[19] M. L. Sehgal, Phys. Rev. **128**, 761 (1962).
[20] R. Van der Linden, F. De Corte, and J. Hoste, J. Radioanal. Chem. **23**, 113 (1974).
[21] R. E. Heft, in *Conference on Computers in Activation Analysis*, edited by R. Farmakes (American Nuclear Society, La Grange Park, IL, 1968).
[22] P. M. Lantz, C. R. Baldock, and L. E. Idom, Nucl. Sci. Eng. **20**, 302 (1964).
[23] J. Alstad, T. Jahnsen, and A. C. Pappas, J. Inorg. Nucl. Chem. **29**, 2155 (1967).
[24] M. D. Ricabarra, R. Turjanski, G. H. Ricabarra, and C. B. Bigham, Can. J. Phys. **46**, 2473 (1968).
[25] E. Steinnes, J. Inorg. Nucl. Chem. **34**, 2699 (1972).
[26] R. Van der Linden, F. De Corte, and J. Hoste, J. Radioanal. Chem. **20**, 695 (1974).
[27] L. P. Roy and L. Yaffe, Can. J. Chem. **34**, 1023 (1956).
[28] E. Browne and J. K. Tuli, Nucl. Data Sheets **108**, 2173 (2007).
[29] E. A. Henry, N. Smith, P. G. Johnson, and R. A. Meyer, Phys. Rev. C **12**, 1314 (1975).
[30] J. R. Huizenga and R. Vandenbosch, Phys. Rev. **120**, 1305 (1960).
[31] X. Ledoux, J. Sigaud, T. Granier, J.-P. Lochard, Y. Patin, P. Pras, C. Varignon, J.-M. Laborie, Y. Boulin, and F. Gunsing, Eur. Phys. J. A **27**, 59 (2006).
[32] K. S. Krane and J. Sylvester, Phys. Rev. C **73**, 054312 (2006).
[33] M. C. Eastman and K. S. Krane, Phys. Rev. C **77**, 024303 (2008).
[34] R. B. Firestone, S. F. Mughabghab, and G. L. Molnár, in *Database of Prompt Gamma Rays from Slow Neutron Capture for Elemental Analysis* (International Atomic Energy Agency, Vienna, 2007), Chap. 5.
[35] M. Kortelahti, A. Pakkanen, M. Piiparinen, T. Komppa, and R. Komu, Nucl. Phys. A **376**, 1 (1982).
[36] S. Chanda *et al*., Nucl. Phys. A **775**, 153 (2006).